International Journal of Thermophysics, Vol. 20, No. 6, 1999

Three-Parameter Corresponding-States Correlations for Joule–Thomson Inversion Curves[1]

M. G. Castillo,[2] C. M. Colina,[2,3] J. E. Dubuc,[2] and C. G. Olivera-Fuentes[2]

In the present work, the Lee–Kesler (LK) and Boublík–Alder–Chen–Kreglewski (BACK) equations of state were used to compute Joule–Thomson inversion curves for nonsimple fluids. Comparisons with available data showed that predictions were quite reliable and could be used in place of experimental values. Two sets of corresponding-states correlations were developed, giving reduced inversion pressures and densities as functions of reduced temperature and acentric factor. The LK-based correlations are valid for $T_r \leqslant 4.0$, giving an average absolute deviation (AAD) of 4.5% for pressures. The BACK-based correlations are valid up to the maximum inversion temperature and give a 6.7% AAD for pressures. Respective volume AADs are 12.0 and 8.0% in the high-density region.

KEY WORDS: correlation; corresponding-states; inversion curve; Joule-Thomson.

1. INTRODUCTION

The passing of a fluid through a restriction, with a drop in pressure, is usually followed by a change in temperature. In an adiabatic process, this change can be quantified by means of the Joule–Thomson coefficient, μ_J, defined as

$$\mu_J = \left(\frac{\partial T}{\partial P}\right)_H \tag{1}$$

[1] Paper presented at the Thirteenth Symposium on Thermophysical Properties, June 22–27, 1997, Boulder, Colorado, U.S.A.

[2] TADiP Group, Thermodynamics and Transport Phenomena Department, Universidad Simón Bolívar, AP 89000, Caracas 1086-A, Venezuela.

[3] To whom correspondence should be addressed.

0195-928X/99/1100-1737$16.00/0

where T is temperature, P is pressure, and H is enthalpy. The Joule–Thomson inversion curve (JTIC) is the locus of thermodynamic states in which the temperature of the fluid is invariant with respect to isenthalpic expansion, $\mu_J = 0$.

As usually represented in pressure–temperature coordinates, the JTIC extends from a minimum temperature corresponding to a saturated state to a maximum temperature corresponding to the ideal-gas limit at zero density and pressure. The curve is parabolic in shape, with a maximum inversion pressure at an intermediate temperature. The inversion curve can also be represented in volume–temperature coordinates but this is less common.

Direct measurement of inversion points is difficult and unreliable. Under near-inversion conditions where the Joule–Thomson coefficient goes to zero, very small temperature differences will result even from very large pressure changes. Hence, extremely accurate temperature measurements are necessary for the inversion pressures to be determined reliably. Thus, the preferred course is the use of thermodynamic relations such as

$$\left(\frac{\partial Z}{\partial T}\right)_P = 0 \tag{2}$$

$$T\left(\frac{\partial P}{\partial T}\right)_v + v\left(\frac{\partial P}{\partial v}\right)_T = 0 \tag{3}$$

(where v is the specific or molar volume, and Z is the compressibility factor) to compute inversion points from experimental PvT data, either by direct numerical differentiation of the raw data or by first fitting them with a high-precision, multiparameter equation of state (EOS). Even then, the complete inversion curves of many fluids cannot be established, as they extend into regions of high temperature or pressure not accessible to experimental measurement.

Efforts have been made to derive generalized inversion curves from the known behavior of the lighter fluids. Gunn et al. [1] computed inversion points from volumetric data available for Ar, Xe, N_2, CO, CH_4, and C_2H_6; since these failed to cover the upper temperature portion of the inversion curve, additional theoretical points were computed for Ar from a three-term truncated virial equation with coefficients based on the Kihara intermolecular potential. Both experimental and calculated data for the JTIC were then correlated using the empirical equation,

$$P_r = -36.275 + 71.598T_r - 41.567T_r^2 + 11.826T_r^3 - 1.6721T_r^4 + 0.091167T_r^5 \tag{4}$$

where P_r is reduced pressure and T_r is reduced temperature. An alternative correlation was proposed by Miller [2] on the basis of inversion data for CO_2, N_2, CO, CH_4, C_2H_6, C_3H_8, Ar, and NH_3 as

$$P_r = 24.21 - \frac{18.54}{T_r} - 0.825 T_r^2 \tag{5}$$

Equations (4) and (5) are two-parameter corresponding-states correlations that should give comparable results, as they are derived from data for the same or very similar, relatively simple fluids. Gunn et al. [1] described the gases as small, nearly spherical molecules whose acentric factors are close to zero, and Miller [2] described them as gases having a critical compressibility factor of approximately 0.29.

The computation of JTICs has long been recognized as a very sensitive test of the predictive capabilities of an equation of state [1–5]. Comparisons of predicted and experimental JTICs can reveal limitations and suggest improvements in the volume and temperature dependences of an EOS. Several authors [2–5] have therefore sought to assess and rank EOS performance by comparing predicted inversion curves and the above empirical correlations; however, the comparison is appropriate only for simple fluids, greatly restricting the scope of the analysis. More general correlations, valid for a wider range of fluids, would clearly be a valuable tool to use in these kinds of studies. Given the scarcity of experimental data for heavy and polar fluids, in the present paper we generate instead inversion curves from two highly reliable multiparameter equations of state and use these as a basis for the development of new correlations not limited to simple fluids.

2. DEVELOPMENT OF NEW CORRELATIONS

2.1. Lee–Kesler Equation of State

The Lee–Kesler (LK) [6] equation,

$$Z = Z^{(0)} + \frac{\omega}{\omega^{(r)}} [Z^{(r)} - Z^{(0)}] \tag{6}$$

is a generalization of the Benedict–Webb–Rubin EOS within the framework of three-parameter corresponding state theory. In Eq. (6), ω is the acentric factor, and superscripts (0) and (r), respectively, denote properties of the simple fluid ($\omega = 0$) and a reference fluid (n-octane; $\omega = 0.3978$). As described by its authors, the LK EOS accurately represents the volumetric

and thermodynamic properties of nonpolar and slightly polar fluids and their mixtures for reduced temperatures from 0.3 to 4 and reduced pressures from 0 to 10. A procedure to compute JTICs from the LK equation was described by Dilay and Heidemann [4], who concluded that this EOS gave the most accurate prediction of inversion curves over the entire temperature range.

2.2. BACK Equation of State

The BACK (Boublík–Alder–Chen–Kreglewski) EOS is an augmented hard-core equation of the form

$$Z = Z^{h} + Z^{a} \tag{7}$$

Equation (7) expresses the compressibility factor of a real fluid as the sum of repulsive (Z^{h}) and attractive (Z^{a}) contributions. Chen and Kreglewski [7] suggested using the polynomial expansion of Alder for the attractive term and the Boublík expression for the repulsive term. This equation has 24 universal constants obtained by Alder et al. [8] by fitting internal energy and PvT data of liquid and gaseous argon. It also contains five parameters characteristic of individual compounds that have to be evaluated from experimental data for each pure substance.

The BACK equation appears particularly attractive for several reasons. It is highly accurate in fitting the PvT behavior of a number of substances [7, 9]. Only a few equation constants are required for each substance, and these are available for 52 compounds in the TRC tables [10]. To the best of our knowledge, the BACK EOS has not been used before to compute inversion curves; however, it has been found to be the most accurate source of residual internal energies [11], heat capacities [12], and enthalpies [13]. It seems reasonable, therefore, to expect that it will yield similarly accurate predictions of JTICs, because these also depend on good representation of the partial derivatives of the $P(T, v)$ function. An additional advantage of this EOS is its wide range of application, which extends at least up to $T_r = 7$ and $P_r = 20$. This last point is very important because most equations of state (including the LK model) do not reach these high values of T_r and P_r, and thus the inversion curves cannot be generated in that range.

2.3. Validation of Inversion Curves

Figure 1 shows inversion curves computed from the correlations of Gunn et al. [1] and Miller [2] and from the LK equation for simple fluids

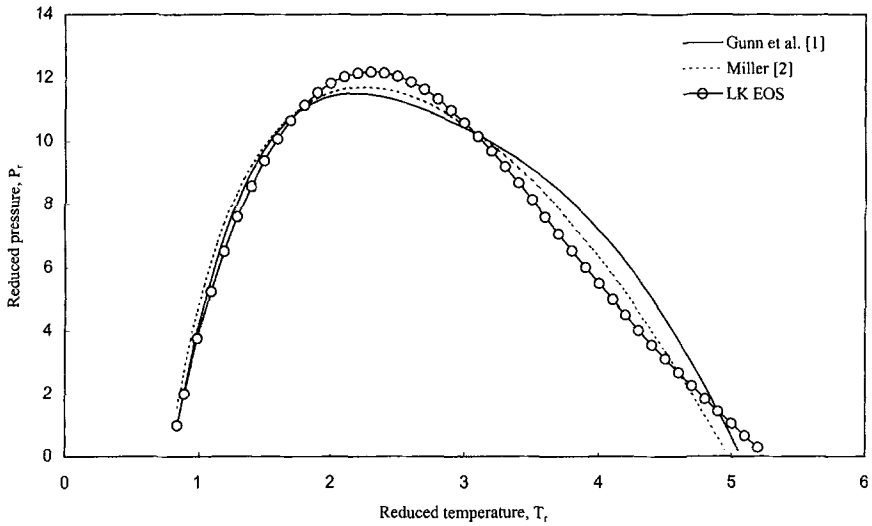

Fig. 1. Inversion curves for simple fluids, computed from the Gunn et al. [1] and Miller [2] correlations and from the Lee–Kesler [6] EOS.

$Z^{(0)}(P_r, T_r)$. It can be seen that both empirical correlations, despite being based on similar experimental data, give somewhat different curves. The discrepancies can be attributed to the different fluids considered in the development of each correlation. The Miller correlation [2] predicts a higher maximum inversion pressure, as a result of including data for heavier or polar compounds such as CO_2, C_3H_8, and NH_3. Differences are also noticeable in the high-temperature region, where the Miller correlation is partly based on experimental data for N_2, whereas the correlation by Gunn et al. [1] makes use of theoretically computed points for Ar. The absolute deviation of reduced pressures between both curves is approximately 12% on average but can be as high as 100% near the end points; these values can be taken as indicative of the general level of precision to be expected from a generalized correlation of inversion curves.

Similar comments apply in Fig. 1 to the inversion curve computed from the LK EOS for simple fluids [6], which was developed mainly from data for Ar, Kr, and CH_4. The largest deviations from the empirical curves occur around the maximum inversion pressure, which exceeds the pressure limit for this EOS, and also in the upper temperature branch of the JTIC above $T_r = 4$, which exhibits a qualitative behavior that deviates from the experimental trend and is shown only for the sake of completeness (although the extrapolation is by no means unreasonable). In the range of validity of the EOS, the predicted inversion curve is in good agreement

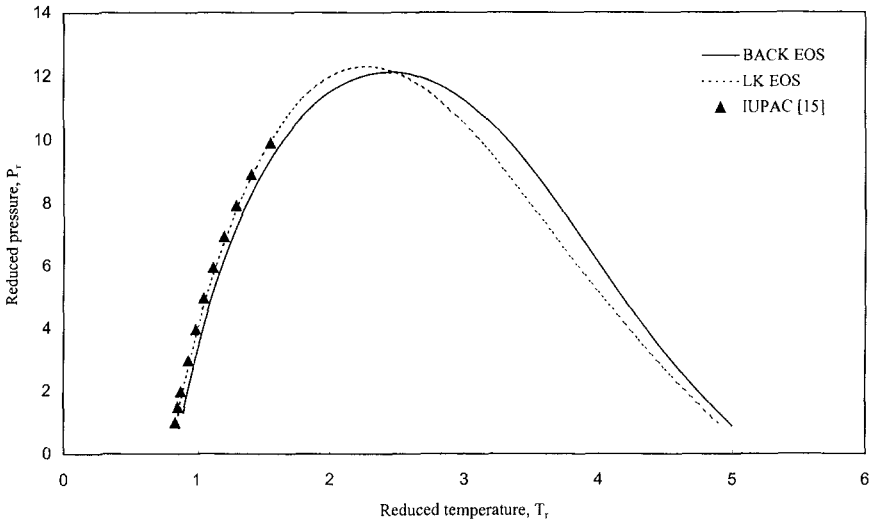

Fig. 2. Inversion curves for oxygen, computed from the BACK and LK EOSs. Points represent values obtained from the IUPAC tables [15].

with the empirical correlations, within the limits of uncertainty referred to above.

Further support for the LK EOS can be obtained from Fig. 2, in which inversion curves predicted for oxygen by the LK EOS (with $\omega = 0.0218$ [14]) and the BACK EOS (with parameters taken from the TRC compilation [10]) are compared with inversion points obtained by interpolation of the IUPAC Tables for this fluid [15]. Both equations of state predict similar inversion curves, again within the expected bounds of precision. The LK EOS is clearly superior at the lower temperatures, but some increase in deviation is evident as temperature increases, consistent with the findings from Fig. 1. Although no reference data are available for comparison at higher temperatures and pressures, it may be expected that the BACK EOS performs better in this region, given its previously mentioned wider range of validity.

The BACK EOS may also give better results for heavier or polar fluids, which typically exhibit higher peak inversion pressures. This is illustrated in Fig. 3, showing inversion curves of ammonia ($\omega = 0.252$ [14]) predicted from both EOSs and reference points obtained by interpolation of Joule–Thomson coefficients reported by Haar and Gallagher [16].

As illustrated by Figs. 2 and 3, experimental inversion data (or data derived from experimental PvT measurements) usually fail to cover the complete span of the inversion curve. These figures nevertheless suggest

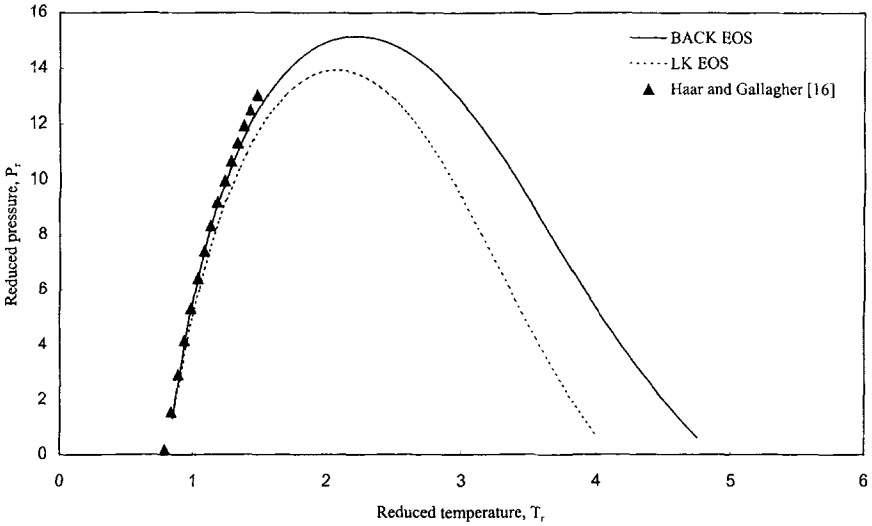

Fig. 3. Inversion curves for ammonia, computed from the BACK and LK EOSs. Points represent values obtained from Haar and Gallagher [16].

that the LK and BACK EOSs can be expected to provide reliable predictions in their respective ranges of validity, even if it is not possible to give a quantitative measure of the errors involved, given the lack of reference data. The average absolute deviation (AAD) of pressures with respect to the available data points is 7.7% for the LK values in Fig. 2 and 5.3% for the BACK values in Fig. 3 but may obviously become larger at higher temperatures. If generalized correlations are in any case to be developed for nonsimple fluids, it is unavoidable to rely on predictions from theoretical models, as was indeed done by Gunn et al. for simple fluids in their already cited work [1]. On the basis of their known performance, we have therefore chosen the LK and BACK EOSs in the present work as the source of inversion curves from which the new correlations will be developed.

2.4. Generalized Correlation of LK Inversion Curves

Inversion curves were computed from the LK EOS with acentric factors ranging from 0.0 to 0.5. The latter value is only slightly higher than the acentric factor of *n*-decane, which was the heaviest hydrocarbon used by Lee and Kesler [6] in the development of their EOS. The following function was found to give the best fit of the P_r–T_r curves:

$$P_r = \sum_{i=0}^{4} (a_i + b_i \omega^{n_i})\, T_r^i \tag{8}$$

Table I. Coefficients for Correlations of LK Inversion Curves, Eqs. (8) and (9)

	$i=0$	$i=1$	$i=2$	$i=3$	$i=4$
a_i	−21.938	37.431	−13.521	1.7906	−0.0800
b_i	−20.355	42.258	−14.355	−0.449	0.336
n_i	0.95	1.04	1.09	1.16	1.20
c_i	1.884	5.133	0.463	−0.716	0.0824
d_i	12.703	−9.701	14.78	−6.482	0.587
m_i	1.2	1.2	1.1	1.1	1.0

with coefficients given in Table I. It may be seen that Eq. (8) resembles Eq. (4), but with coefficients that are now functions of the acentric factor. A fifth-degree polynomial was also tried but actually gave worse results than the fourth-degree formula of Eq. (8).

Figure 4 shows inversion curves computed from Eq. (8) for acentric factors ranging from 0.0 to 0.5. Sample points computed from the LK EOS for the simple and reference fluids are also plotted in this figure, to illustrate the general degree of agreement achieved in the correlation. Although the present correlation is intended for $T_r \leqslant 4.0$ only, corresponding to the temperature limit for application of the LK model, JTICs in Fig. 4

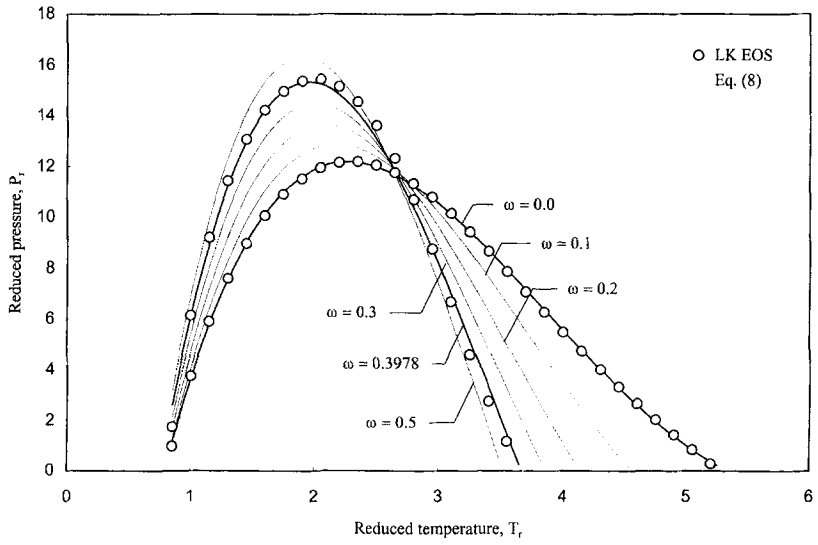

Fig. 4. Inversion curves for normal fluids, computed from Eq. (8) developed in this work. Points represent actual LK values for the simple and reference fluids.

extend beyond $T_r = 4.0$, once again, for the sake of completeness and, also, to show that extrapolation of Eq. (8) continues to give an excellent representation of LK inversion curves. The AAD of reduced pressures between Eq. (8) and LK values is 4.5% over the entire range of acentric factors involved.

It is interesting to point out that, unlike the first-order corresponding-states principle implied by Eq. (6), the coefficients of the present correlation are not linear functions of acentric factor. This nonlinearity should be evident from Fig. 4, where inversion pressures can be seen to increase with increasing acentric factor at low temperatures but exhibit the opposite trend at high temperatures. In fact, the inversion curves predicted by the LK EOS for the simple and reference fluids intersect at approximately $T_r = 2.72$ and $P_r = 11.59$; as a consequence, all other inversion curves predicted by this EOS must pass through this same point. The correlation of Eq. (8) was not constrained to reproduce this feature exactly.

Computation of inversion points from pressure-explicit equations of state usually involves iteration on volumes at a given temperature until the inversion criterion, e.g., Eq. (3), is satisfied. It would be useful in this respect to have available a generalized volume–temperature correlation of inversion curves, which, at the very least, could serve to generate good initial estimates of inversion volumes. Since molar volume becomes unbounded at the maximum inversion temperature, where pressure goes to zero and the fluid approaches ideal-gas behavior, we used molar inversion densities computed from the LK EOS to establish the following correlation:

$$\frac{RT_c}{P_c}\rho = \sum_{i=0}^{4} (c_i + d_i \omega^{m_i})\, T_r^{i-1} \tag{9}$$

with coefficients given also in Table I. The dimensionless density in the left-hand side of Eq. (9), containing critical temperature T_c, critical pressure P_c, and molar density ρ, is the reciprocal of the volume variable v_r used by Lee and Kesler [6]. This correlation is subject to the same limits of application as Eq. (8), and the AAD of volumes over the entire range of acentric factors is 12.0% for dimensionless densities greater than 0.33 ($v_r < 3$). Relative errors increase at lower densities, as should be expected because densities go to zero.

2.5. Generalized Correlation of BACK Inversion Curves

Inversion curves were generated for the 52 compounds whose BACK parameters are available in the TRC tables [10]. Analysis of the JTICs obtained for alcohols suggested that the BACK EOS yields much less

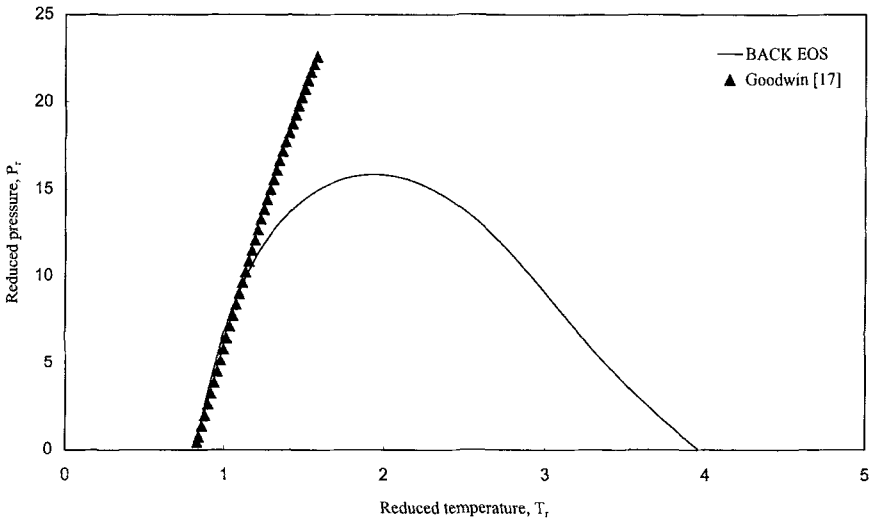

Fig. 5. Inversion curve for methanol, computed from the BACK EOS. Points represent values obtained from Goodwin [17].

accurate predictions for these fluids. This is illustrated by Fig. 5, where the predicted inversion curve for methanol is compared with the set of inversion points reported by Goodwin [17]. Prediction of JTICs for these strongly polar fluids involves extrapolation of the EOS to very high reduced pressures and is unlikely to be successful even for complex EOS models, e.g., the IUPAC EOS for methanol [18] similarly fails to reproduce the Goodwin data when extrapolated beyond $T = 600$ K ($T_r = 1.17$). Given these considerations, alcohols were excluded from the present correlations, because their computed inversion curves were anticipated to deviate from true fluid behavior, especially at high temperatures.

Following the TRC classification of compounds as hydrocarbons and nonhydrocarbons, separate correlations were developed for the pressure–temperature and volume–temperature inversion curves of these two classes of fluids. The best results were obtained using the same Eqs. (8) and (9), with the coefficients given in Table II. It may be noted that in most cases the dependence of the coefficients on acentric factor could be fitted by a single constant exponent. The P_r–T_r correlations are valid from the minimum to the maximum inversion temperature for all hydrocarbons and nonhydrocarbons; the v_r–T_r correlations are valid only up to $v_r = 3$.

Figure 6 shows inversion curves in P_r–T_r coordinates for cumene, calculated with the BACK EOS and with the present correlation. An analogous comparison of inversion curves in v_r–T_r coordinates is presented

Table II. Coefficients for Correlations of BACK Inversion Curves, Eqs. (8) and (9)

	$i=0$	$i=1$	$i=2$	$i=3$	$i=4$
			Hydrocarbons		
a_i	−20.338	36.096	−12.478	1.4541	−0.0482
b_i	−42.815	85.759	−47.575	9.5410	−0.6465
n_i	2.0	2.0	2.0	2.0	2.0
c_i	4.5347	1.6017	2.6438	−1.2746	0.1290
d_i	0.0933	−0.0599	0.3496	−0.1825	0.02267
m_i	−1.4	−1.1	−0.50	−0.50	−0.52
			Nonhydrocarbons		
a_i	−16.697	28.661	−8.7013	0.7553	−0.0046
b_i	−40.947	83.101	−44.114	8.573	−0.5662
n_i	1.3	1.3	1.3	1.3	1.3
c_i	4.0529	1.4470	2.4906	−1.1311	0.1096
d_i	8.0403	2.2561	5.0673	−3.8789	0.5276
m_i	1.8	1.8	1.8	1.8	1.8

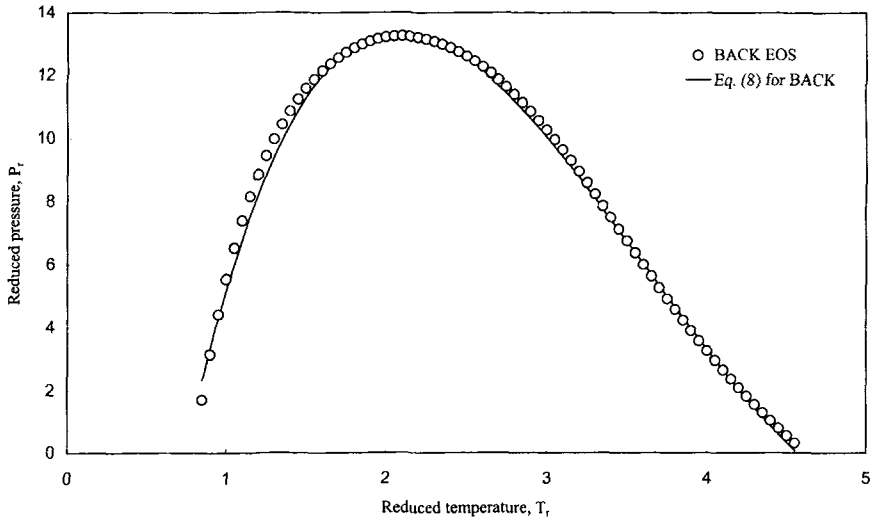

Fig. 6. Inversion curves (P_r-T_r) for cumene, computed from the BACK EOS and from Eq. (8).

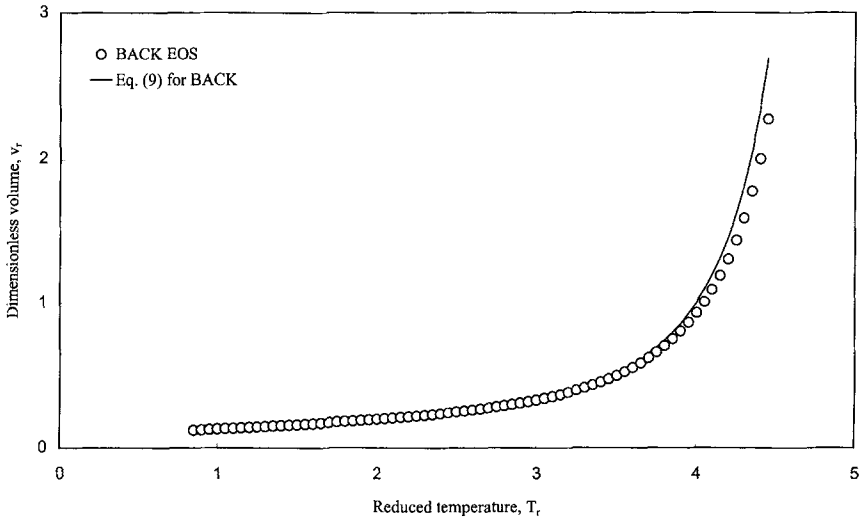

Fig. 7. Inversion curves (v_r–T_r) for cyclohexane, computed from the BACK EOS and from Eq. (9).

in Fig. 7 for cyclohexane. Similar results were obtained for all fluids, with AADs of 6.7% for pressures and 8.0% for volumes. A more detailed comparison is given in Table III, where pressure and volume AADs are listed for each of the 48 compounds studied.

Table III. AAD for Correlations Obtained from the BACK EOS

Substance	ω^a	AAD[b]	
		P_r–T_r	v_r–T_r
Hydrocarbons			
Methanethiol	0.1460	3.96	12.30
1-Butene	0.1867	2.85	7.36
Isobutene	0.1893	2.68	7.89
Ethanethiol	0.1921	3.34	7.62
Thiophene	0.1928	2.33	6.51
Tetrahydrothiophene	0.1988	6.29	6.74
Benzene	0.2108	4.25	6.51
Cyclohexane	0.2118	4.35	7.10
Propyne	0.2161	8.25	9.14
Methylcyclohexane	0.2350	3.16	7.15

Table III. *(Continued)*

Substance	ω^a	AAD[b] P_r–T_r	AAD[b] v_r–T_r
trans-Decahydronaphthalene	0.2536	11.76	14.29
Toluene	0.2641	4.22	3.63
cis-Decahydronaphthalene	0.2942	7.40	11.36
Naphthalene	0.3019	7.55	3.24
n-Hexane	0.3046	10.00	1.46
m-Xylene	0.3086	6.21	9.44
o-Xylene	0.3127	4.38	10.57
p-Xylene	0.3259	3.92	9.44
Tetralin	0.3278	11.08	1.95
Cumene	0.3377	3.78	10.15
n-Heptane	0.3511	6.26	9.17
1,1-Biphenyl	0.3659	22.23	22.71
p-Xymene	0.3722	7.53	11.15
Isooctane	0.3769	8.92	13.38
n-Octane	0.3962	14.75	9.48
n-Nonane	0.4377	9.37	14.24
n-Decane	0.4842	6.95	15.82
Nonhydrocarbons			
Oxygen	0.0218	1.39	0.76
Hydrogen sulfide	0.0827	2.09	1.70
Trichlorofluoromethane [20]	0.189	3.40	11.69
Chlorotrifluoromethane [20]	0.198	3.75	6.11
Furan	0.1997	2.70	2.58
Dichlorodifluoromethane [20]	0.204	6.24	8.30
Dichlorofluoromethane	0.2069	3.37	5.04
Chlorodifluoromethane	0.2192	2.19	2.57
Tetrahydrofuran	0.2264	4.86	1.54
1,1-Dichloro-1,2,2,2-tetrafluoroethane [20]	0.2366	9.78	3.90
Sulfur dioxide	0.2451	4.38	4.00
1,2-Dichloro-1,1,2,2-tetrafluoroethane [20]	0.246	8.75	10.55
Difluoroethane [20]	0.256	12.11	9.40
1,1,2-Trichloro-1,2,2-trifluoroethane [20]	0.256	7.21	9.23
Trifluoromethane [20]	0.26	6.14	3.74
t-Butyl methyl ether	0.2674	3.59	6.67
Methanamine	0.2813	6.79	5.51
Diethyl ether	0.2846	2.09	4.34
Isoquinoline	0.2885	2.15	4.44
2-Propanone	0.3064	18.24	11.22
Quinoline	0.3287	7.08	5.71

[a] Taken from Ref. 14, except for halocarbons marked otherwise.
[b] ABS[$\sum$(BACK − CORR)/BACK] * (100/N).

3. COMMENTS AND CONCLUSIONS

Generalized corresponding-states correlations have been developed for Joule–Thomson inversion curves (P_r–T_r and v_r–T_r) as functions of the reduced temperature and acentric factor. In the absence of a sufficiently extensive inversion database, the reliable BACK and LK equations, valid for a wide range of fluids, were used to generate the necessary inversion points. Given this lack of experimental data, it is not possible to quantify the errors of the present correlations with respect to real values. However, good agreement may be expected in the region where data is available, as shown, for example, in Figs. 8 and 9, where inversion curves for benzene ($\omega = 0.2108$ [14]) computed from the new correlations are compared with data reported by Goodwin [19]. In P_r–T_r coordinates, the LK- and BACK-based correlations give pressure AADs of 4.9 and 12.6%, respectively; in v_r–T_r coordinates, volume AADs are 15.0 and 9.3%, respectively. Once again, these comparisons are limited by the fact that the reference data cover only a fraction of the inversion curve, in this case up to $T = 1200$ K ($T_r = 2.1$) for this compound.

The new correlations are recommended for use in testing simpler, e.g., cubic EOS models, especially for nonsimple fluids whose acentric factor differs significantly from zero, for which previously available correlations [1, 2] would be inadequate.

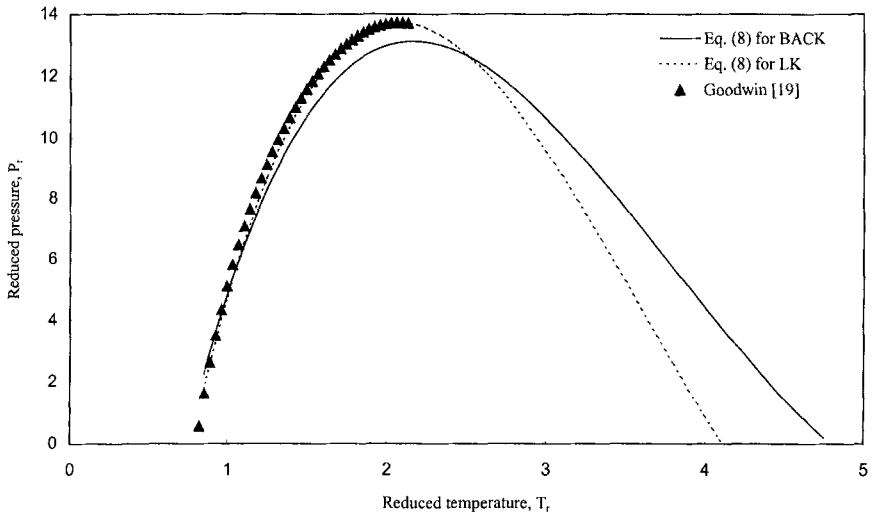

Fig. 8. Inversion curves (P_r–T_r) for benzene, computed from the new correlations. Points represent values obtained from Goodwin [19].

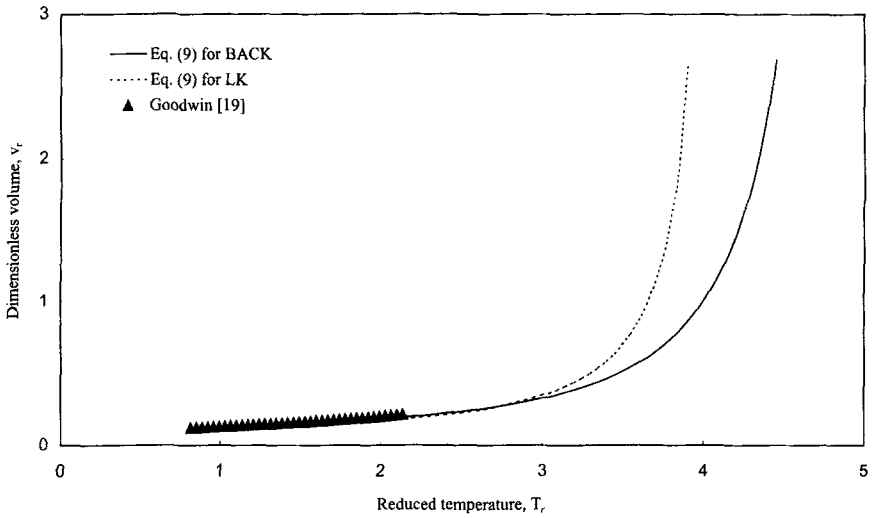

Fig. 9. Inversion curves (v_r–T_r) for benzene, computed from the new correlations. Points represent values obtained from Goodwin [19].

REFERENCES

1. R. D. Gunn, P. L. Chueh, and J. M. Prausnitz, *Cryogenics* **6**:324 (1966).
2. D. G. Miller, *Ind. Eng. Chem. Fundam.* **9**:585 (1970).
3. K. Juris and L. A. Wenzel, *AIChE J.* **18**:152 (1972).
4. G. W. Dilay and R. A. Heidemann, *Ind. Eng. Chem. Fundam.* **25**:152 (1970).
5. A. V. Colazo, F. A. Da Silva, E. A. Müller, and C. Olivera-Fuentes, *Lat. Am. Appl. Res.* **22**:135 (1992).
6. B. I. Lee and M. G. Kesler, *AIChE J.* **21**:510 (1975).
7. S. S. Chen and A. Kreglewski, *Ber. Bunsenges Phys.* **81**:1048 (1977).
8. B. J. Alder, D. A. Young, and M. A. Mark, *J. Chem. Phys.* **56**:3013 (1972).
9. J. J. Simnick, H. M. Lin, and K. C. Chao, *Adv. Chem. Ser.* **182**:209 (1979).
10. Thermodynamic Research Center, *TRC Thermodynamic Tables* (Texas A&M University System, College Station, 1989).
11. J. M. Shaw and J. Lielmezs, *Chem. Eng. Sci.* **40**:1793 (1985).
12. D. Garipis and M. Stamatoudis, *AIChE J.* **38**:302 (1992).
13. T. Manavis, M. Volotopoulos, and M. Stamatoudis, *Chem. Eng. Commun.* **130**:1 (1994).
14. T. E. Daubert and R. P. Danner, *Thermodynamic Properties of Pure Chemicals* (Hemisphere, Washington, DC, 1988).
15. W. Wagner and K. M. de Reuck, *Oxygen*, International Thermodynamic Tables of the Fluid State—9 (Blackwell Scientific, Oxford, 1987).
16. L. Haar and J. S. Gallagher, *J. Phys. Chem. Ref. Data* **7**:635 (1978).
17. R. D. Goodwin, *J. Phys. Chem. Ref. Data* **16**:799 (1987).
18. K. M. de Reuck and R. J. B. Craven, *Methanol*, International Thermodynamic Tables of the Fluid State—12 (Blackwell Scientific, Oxford, 1993).
19. R. Goodwin, *J. Phys. Chem. Ref. Data* **17**:4 (1988).
20. M. J. Lee and Y. L. Chao, *Fluid Phase Equil.* **67**:111 (1991).